

Behaviour of FRP - to - concrete bonded joints

W. (Karu) Karunasena and K. Williams
School of Engineering, James Cook University
Townsville, Queensland 4811, Australia
Email: Karu.Karunasena@jcu.edu.au

Abstract

The bond behaviour between FRP (fibre-reinforced polymer) and concrete is a consideration in the design of FRP strengthening mechanisms for structurally deficient or functionally obsolete concrete structures. In the past, a number of empirical models and fracture mechanics based theoretical models have been proposed for determining the effective bond length and bond strength of FRP sheets/plates bonded to concrete. However, these methods have yielded large discrepancies in the predictions of effective bond length and bond strength. In this paper, the results of an experimental investigation into effective bond length and bond strength are presented. Comparison of experiments results with predictions from three empirical and three fracture mechanics based theoretical models shows that a recently proposed fracture mechanics based local-bond slip model provides a conservative prediction of the effective bond length and an accurate prediction of bond strength.

1. Introduction

The bonding of external FRP sheets/plates (referred to as plates only hereafter) to reinforced concrete (RC) beam members to provide increased strength is emerging as a popular strengthening practice due to several useful aspects of FRP such as high strength, corrosion resistance, long term durability and simplicity in application to existing structures¹. During the load distribution process, externally applied FRP plates act like tension reinforcement. A major concern in the use of FRP in the structural design is the pre-mature debonding or delamination of FRP plate from the RC beam, caused by crack propagation parallel to the bonded plate near or along the adhesive/concrete interface.

Previous research^{2,3} has shown that there are two basic debonding types or modes in FRP strengthened beam members: *end debonding* and *midspan debonding*. End debonding originates near the plate end and propagates along or near the bondline. Midspan debonding originates at the intersection of the FRP plate and a flexural crack or flexural shear crack in concrete and then propagate along the bondline towards the plate ends. For the two basic debonding modes, the stress state of the interface is similar to that in a pull test in which a FRP plate is bonded to a concrete prism and is subject to tension as shown in Figure 1. As a

result, a number of experimental and theoretical studies^{4,7} have been carried out to investigate the FRP-to-concrete bond behaviour in pull tests. These studies suggest that there exists an effective bond length beyond which an extension of the bond length cannot increase the ultimate load (referred to as the bond strength hereafter) in FRP-to-concrete bonded joints.

In the past, a number of empirical models and fracture mechanics based theoretical models have been proposed for determining the effective bond length and the bond strength. However, the applicability of these strength models in the design of the strengthening systems is still not conclusive as different models have yielded significantly different results for the effective bond length and the bond strength. This paper presents the results of an experimental investigation into effective bond length and bond strength in pull tests in which a Carbon fibre-reinforced polymer plate (CFRP) is bonded to a concrete prism. A comparison of present experimental results with predictions from three empirical and three fracture mechanics based theoretical models is also presented.

2. Testing Program

Figure 1 shows the schematic diagram of the pull test setup adopted in this study. The test consists of a CFRP plate appropriately attached

to a rectangular concrete prism of specified dimensions (in this study 150x150x350 mm). Degussa Construction Chemicals⁸ in Australia supplied all FRP materials (ie Mbrace CFRP Laminate 150/2000, Mbrace Primer, Mbrace Laminate adhesive and MBT Thinner No. 1), and their guidelines were followed when bonding the CFRP plates to concrete prisms. The CFRP used had a modulus of elasticity of 165 GPa, a width of 50 mm and an average thickness of 1.3 mm. The average concrete cylinder strength was 32 MPa.

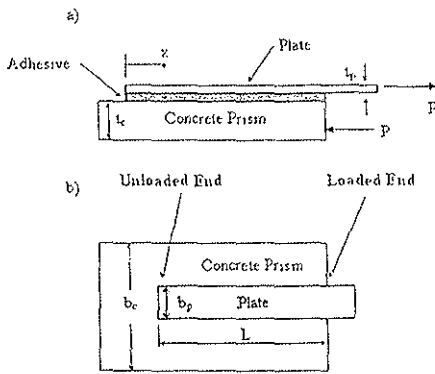


Figure 1: Schematic Diagram of Pull Test Set-up (a) Elevation (b) Plan

In the test set-up, the concrete prism is restrained in a vertical position inside an MTS machine (Universal compressive and tensile hydraulic testing machine) by a unique brace and the overhang of FRP plate is attached to the uppermost arm in the MTS machine. With both the FRP plate and the concrete prism sufficiently braced, the MTS machine incrementally applies an axial tensile load to the FRP plate, resulting in a shear stress distribution in the bond.

To determine the effective bond length experimentally, twenty five concrete prism specimens were prepared and CFRP plates were bonded to them in such a way that bond length (L) was increased from 100 mm to 300 mm in increments of 50 mm, giving 5 specimens of CFRP plated concrete prisms for each bond length. Then each specimen was tested in the MTS machine by gradually increasing the load on the CFRP plate until the CFRP plate dislodged from the concrete prism. The ultimate failure load (bond strength) P_u , for each specimen was recorded.

3. Strength Prediction Models

Several models have been proposed to predict the effective bond length (L_e) and the bond strength in FRP-to-concrete bonded joints. Some of these are empirical models developed based on the observed experimental results and others have been developed using the fracture mechanics theory. For brevity, only three empirical and three fracture mechanics theory based models are presented here.

3.1 Empirical Models

Model 1 –Maeda et al. Model

Maeda et al.^{4,9} proposed an empirical model for effective bond length and bond strength based on test results. Their model is represented by

$$L_e = e^{6.13-0.58 \ln(0.001 E_p t_p)} \quad (\text{mm}) \quad (1a)$$

$$P_u = \frac{110.2}{10^6} L_e b_p E_p t_p \quad (\text{N}) \quad (1b)$$

where E_p is the Young's modulus of FRP plate in MPa and all length terms are as defined in Figure 1. Length units of mm should be used in this equation. This model is valid for $L \geq L_e$ only.

Model 2 –Khalifa et al. Model

Khalifa et al.¹⁰ modified Maeda model to include the effect of concrete compressive strength by replacing equation (1b) with

$$P_u = \frac{110.2}{10^6} \left(\frac{f'_c}{42} \right)^{2/3} L_e b_p E_p t_p \quad (\text{N}) \quad (2)$$

where f'_c is the cylinder concrete compressive strength in MPa and effective length is given by equation (1a).

Model 3 –Iso Model

Iso⁶ proposed the following bond strength model:

$$L_e = 0.125 (E_p t_p)^{0.57} \quad (\text{mm}) \quad (3a)$$

$$P_u = 0.93L_c b_p (f_c')^{0.44} \quad (\text{N}) \quad (3b)$$

where $L_c = L$ if $L_c > L$. Herein, E_p is in MPa and all length terms are in mm.

3. Fracture Mechanics based Models

Model 4 – Neubauer and Rostasy model

Through the use of nonlinear fracture mechanics Holzenkampfer⁴ studied the relationship between steel plate reinforcement and concrete. He attempted to derive the ultimate failure load expression based on the knowledge of the effective bond length dependency, resulting in two separate expressions for $L \geq L_c$ and $L < L_c$. Later, Neubauer and Rostasy¹¹ modified this model for the use of both steel and FRP reinforcement. The modified expressions for L_c (mm) and P_u (N) are given by

$$L_c = \sqrt{\frac{E_p t_p}{2f_t}} \quad (4a)$$

$$P_u = 0.64k_p b_p \sqrt{E_p t_p f_t} \quad \text{for } L \geq L_c \quad (4b)$$

$$P_u = 0.64k_p b_p \sqrt{E_p t_p f_t} \frac{L}{L_c} \left(2 - \frac{L}{L_c}\right) \quad \text{for } L < L_c \quad (4c)$$

where E_p is in MPa and all length terms are in mm; f_t (MPa) is the surface tensile strength; and k_p describes a relationship between the width of the reinforcing plate b_p (mm) and the width of concrete prism b_c (mm) expressed as

$$k_p = \sqrt{1.125 \frac{2 - b_p/b_c}{1 + b_p/400}} \quad (4d)$$

Model 5 – Chen and Teng Model

Based on acquired knowledge from previous studies and an in depth analysis of single and

double shear tests, Chen and Teng⁴ developed a model based on cylinder concrete compressive strength f_c' as opposed to the surface tensile strength f_t adopted in model 4. This model provides a more practical analysis due to the fact that f_c' is more readily available than f_t . In this model, L_c (mm) and P_u (N) are given by

$$L_c = \sqrt{\frac{E_p t_p}{\sqrt{f_c'}}} \quad (5a)$$

$$P_u = 0.427 \beta_p \beta_L \sqrt{f_c'} b_p L_c \quad (5b)$$

$$\text{where } \beta_p = \sqrt{\frac{2 - b_p/b_c}{1 + b_p/b_c}}; \quad (5c)$$

$$\text{and } \beta_L = 1 \text{ if } L \geq L_c \quad (5d)$$

$$\beta_L = \sin \frac{\pi L}{2L_c} \text{ if } L < L_c. \quad (5e)$$

In these expressions E_p and f_c' are in MPa and all length terms are in mm.

Model 6 – Lu et al. Model

Recently, Yuan et al.⁵ presented an analytical solution, based on a bi-linear bond-slip model, for the full range behaviour of FRP-to-concrete bonded joints. Later, Lu et al.⁶ presented a refined model, which is essentially a hybrid of Cheng and Teng model (model 5) and analytical solution of Yuan et al. In this refined model, P_u (N) is given by

$$P_u = \beta_L b_p \sqrt{2E_p t_p G_p} \quad (6a)$$

where β_L is given by equations (5d) and (5e), and the interfacial fracture energy G_p is given by

$$G_p = 0.308 \beta_w^{2/3} \sqrt{f_t} \quad (6b)$$

where

$$\beta_w = \sqrt{\frac{2.25 - b_p/b_c}{1.25 + b_p/b_c}} \quad (6c)$$

The effective bond length L_e (mm) is given by

$$L_e = a + \frac{1}{2\lambda_1} \ln \frac{\lambda_1 + \lambda_2 \tan(\lambda_2 a)}{\lambda_1 - \lambda_2 \tan(\lambda_2 a)} \quad (6d)$$

where

$$\lambda_1 = \sqrt{\frac{\tau_{\max}}{s_0 E_p f_p}} \quad (6e)$$

$$\lambda_2 = \sqrt{\frac{\tau_{\max}}{(s_f - s_0) E_p f_p}} \quad (6f)$$

$$a = \frac{1}{\lambda_2} \arcsin \left[0.97 \sqrt{\frac{s_f - s_0}{s_f}} \right], \quad (6g)$$

and

$$\tau_{\max} = 1.5 \beta_w f_t \quad (6h)$$

$$s_0 = 0.0195 \beta_w f_t \quad (6i)$$

$$s_f = \frac{2G_p}{\tau_{\max}} \quad (6j)$$

In equation (6), E_p , f_t and τ_{\max} are in MPa, and all length terms are in mm.

4. Results and Discussion

Experimental values of bond strengths corresponding to different bond lengths are reported in Table 1. To determine the effective bond length, the mean bond strength for each bond length has been plotted against the bond length in Figure 2. This figure shows that as the bond length increases, so too does the corresponding bond strength up to $L=200$ mm. However, for bond lengths beyond 200 mm there is not much variation in the bond strength. Therefore, for the specific geometry considered here, the experimental effective bond length can be taken as approximately 200 mm, which produces a bond strength of approximately 30 kN.

Table 1: Experimental bond strength P_u

for different values of bond length L .

Specimen	L (mm)	P_u (kN)	Mean P_u (kN)
1A	100	23.11	22.1
1B		22.36	
1C		19.27	
1D		22.55	
1E		23.20	
2A	150	27.90	27.4
2B		27.55	
2C		28.45	
2D		28.07	
2E		25.21	
3A	200	32.50	30.7
3B		30.36	
3C		30.08	
3D		28.49	
3E		32.25	
4A	250	28.95	29.4
4B		29.04	
4C		29.62	
4D		30.18	
4E		29.02	
5A	300	27.78	28.9
5B		29.86	
5C		29.57	
5D		28.63	
5E		28.52	

Note: For all specimens, $b_p = 50$ mm, $b_c = 150$ mm and $t_p = 1.3$ mm.

Predictions of effective bond length and bond strength were made using the three empirical models (model 1 to 3) and the three fracture mechanics based models (model 4 to 6) presented in the previous section. In these calculations, the tensile strength f_t was taken as the flexural tensile strength determined from AS3600¹² (ie $f_t = 0.6\sqrt{f_c}$ where both strength units are in MPa). A comparison of experimental effective bond length with predictions from six models is given in Table 2. This table shows that first two empirical models grossly underestimate the effective bond length whereas third empirical model (ie model 3) underestimates the effective bond length by around a third. All three fracture mechanics

based models (models 4 to 6) predicts the effective bond length reasonably accurately while Teng and Cheng model has produced more accurate results. The more comprehensive Lu et al. model (model 6) has overestimated the effective bond length by 19%. However, the prediction from model 6 is conservative and thus it is suitable in the design process.

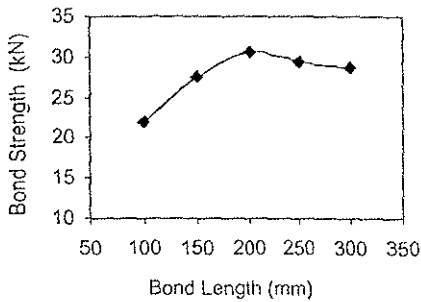


Figure 2: Experimental Bond Strength Vs Bond Length.

Table 2: Comparison of effective bond length L_e from various methods.

Method	L_e (mm)
Experimental	200 (0%)
Model 1 (Maeda et al.)	20 (-90%)
Model 2 (Khalifa et al.)	20 (-90%)
Model 3 (Iso)	137 (-32%)
Model 4 (Neubauer and Rostasy)	178 (-11%)
Model 5 (Teng and Cheng)	195 (-3%)
Model 6 (Lu et al.)	238 (19%)

Note: Percentage difference with respect to experimental value is given within parenthesis.

Table 3 shows the predictions of bond strength from six models along with experimental values for different values of bond length. A graphical representation of the same results can be seen in Figure 3. It is seen that empirical model 3 predicts the bond strength fairly accurately whereas other two empirical models (models 1 and 2) do provide satisfactory predictions. However, it is noted that model 3 underestimated the effective bond length by 32%. Out of the fracture mechanics based models, the Neubauer and Rostasy model (model 4) significantly overestimates the bond strength. The other two fracture mechanics based models (models 5 and 6) closely predict the bond strength but model 6 (Lu et al. model)

seems to provide more accurate results. Moreover, it has been found by other researchers that the ratio of FRP width to concrete width has some influence on the behaviour of the FRP-to-concrete joints. The three fracture mechanics based models considered here take this width ratio into account whereas the three empirical models do not have the concrete prism width coming into their prediction equations. Overall, model 6 provides a conservative estimate of effective bond length and an accurate prediction of the bond strength.

Table 3: Comparison of bond strength P_u from various methods.

Method	P_u (kN)				
	Bond Length L (mm)				
	100	150	200	250	300
Experimental	22.1	27.4	30.7	29.4	28.9
Model 1	24.1	24.1	24.1	24.1	24.1
Model 2	20.1	20.1	20.1	20.1	20.1
Model 3	21.4	29.2	29.2	29.2	29.2
Model 4	28.5	34.4	35.2	35.2	35.2
Model 5	19.0	24.6	26.3	26.3	26.3
Model 6	18.3	25.0	28.9	29.9	29.9

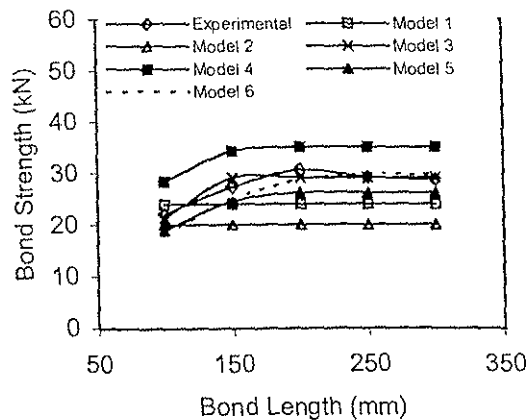


Figure 3: Bond strength from various methods Vs. bond length.

8. Conclusions

In this study, the authors investigated the behaviour of FRP-to-concrete bonded joints in reinforced concrete applications. The main focus was to assess the accuracy of the effective bond

length and bond strength predictions from three empirical and three fracture mechanics based models by comparing with authors' experimental results. Twenty five concrete prisms with carbon fibre-reinforced polymer plates bonded on to a longitudinal side surface of the prisms were tested in a pull test set-up to determine the experimental values of effective bond length and bond strength.

Comparison of experimental results with theoretical predictions indicated that three empirical models considered in this work did not provide an accurate prediction of the effective bond length. However, one of the empirical models closely predicted bond strength. Two of the fracture mechanics based theoretical models provided close predictions of both effective length and bond strength. One of these two models (the Lu et al. model) appear to be suitable for use in the design of FRP strengthening mechanism, as it provides a conservative prediction of effective bond length and an accurate prediction of bond strength.

Authors Biography

Dr W. (Karu) Karunasena is a senior lecturer in civil engineering at James Cook University, Townsville, Australia. He has been involved in fibre composite research for the last 15 years. His current research interests are: rehabilitation and retrofitting of concrete, timber and steel structures using composite materials; non-destructive characterization of material properties and flaws in composite structures; and soil-structure interaction. Mr K. Williams is a civil engineering graduate from James Cook University.

References

1. Teng, J.G., Chen, J.F., Smith, S.T., and Lam, L. FRP strengthened RC structures. UK: John Wiley & Sons; (2002).
2. Pham, H. and Al-Mahaidi, R. Assessment of available prediction models for the strength of FRP retrofitted RC beams. *Composite Structures* (2004), 66, 601-610.
3. Pham, H. and Al-Mahaidi, R. Prediction models for debonding failure loads of carbon fibre reinforced polymer retrofitted reinforced concrete beams. *Journal of Composites for Construction, ASCE* (2006), 10(1), 48-59.
4. Cheng, J.F. and Teng, J.G. Anchorage strength models for FRP and steel plates bonded to concrete. *Journal of Structural Engineering, ASCE* (2001), 127(7), 784-791.
5. Yuan, H. Teng, J.G., Seracino, R., Wu, Z.S. and Yao, J. Full range behaviour of FRP-to-concrete bonded joints. *Engineering Structures* (2004), 26, 553-565.
6. Lu, X.Z., Teng, J.G., Ye, L.P. and Jiang, J.J. Bond-slip models for FRP sheets/plates bonded to concrete. *Engineering Structures* (2005), 27, 920-937.
7. Lu, X.Z., Ye, L.P., Teng, J.G. and Jiang, J.J. Meso-scale finite element model for FRP sheets/plates bonded to concrete. *Engineering Structures* (2005), 27, 564-575.
8. Degussa Construction Materials - <http://www.mbtas.com.au>
9. Maeda, T., Asano, Y., Sato, Y., Ueda, T., and Kakuta, Y. A study on bond mechanism of carbon fiber sheet. Non-metallic (FRP) reinforcement for concrete structures, Proc. of 3rd Int. Symp. Japan Concrete Institute, Sapporo (1997), 1, 279-285.
10. Khalifa, A., Gold, W. J., Nanni, A., and Aziz, A. Contribution of externally bonded FRP to shear capacity of RC flexural members. *Journal of Composites for Construction, ASCE* (1998), 2(4), 195-203.
11. Neubauer, U., and Rostasy, F.S. Design aspects of concrete structures strengthened with externally bonded CFRP plates. Proc., 7th Int. Conf. on Struct. Faults and Repairs, ECS Publications, Edinburgh, Scotland (1997), 2, 109-118.
12. AS3600: Australian Standard for Concrete Structures, Standards Australia (2001)